ELSEVIER

Chemical Engineering Journal 77 (2000) 153–164

Chemical Engineering Journal

www.elsevier.com/locate/cej

Effect of process modeling on the nonlinear behaviour of a CSTR Reactions A→ B→ C

Ana Elisa Gamboa-Torres, Antonio Flores-Tlacuahuac *

Chemical Engineering Department, Universidad Iberoamericana, Prolongación Paseo de la Reforma 880, México DF 01210, Mexico

Received 1 January 1999; received in revised form 5 October 1999; accepted 22 October 1999

Abstract

In this work the nonlinear behaviour of a CSTR in which two exothermic irreversible first-order reactions in series A→ B → C take place, when the jacket energy balance is incorporated in the CSTR mathematical model, is analyzed. Catastrophe theory is used to study the parameters with respect to which output multiplicities, input multiplicities, isola formation and disjoint bifurcations may exist. One main objective of this work is to address the effect of including the jacket energy balance on the nonlinear behaviour of the CSTR. The results show that the steady-state open-loop nonlinear behaviour of CSTRs, modeled without and with the jacket energy balance, is quite different. Using the software XPP-AUTO different bifurcation maps were obtained. Five operating regions were characterized.

Keywords: Input multiplicity; Output multiplicity; Isolas; Disjoint regions; Modeling

1. Introduction

Continuous stirred tank reactors (CSTRs) generally present operational problems due to complex open-loop nonlinear behaviour in the form of input/output multiplicities, ignition/extinction phenomena, Hopf bifurcations, isola formation and disjoint bifurcations. Some of these phenomena had been discussed by Aris [1]. These nonlinear characteristics prove the need and the complexity of the control system design. Results from nonlinear analysis could be important in order to detect potentially difficult operating points and to remove them. For instance, in some cases it may be convenient to operate around an unstable operating point embedded in a multiplicity region. Operation on this unstable point could be convenient because product yields might be higher there. However multiplicity patterns might be different depending upon modeling assumptions. For instance this means that, even using the same set of parameter values, a CSTR modeled without and with the jacket energy balance may result in different multiplicity patterns. This behaviour has been stressed by Russo and Bequette [10].

Input multiplicities arise when different values of a manipulated variable (variable chosen as system input) produce the same value of the variable chosen as system output. One problem that may occur when there are input multiplicities is the possible transition from one steady state to another steady state without detecting it [8]. This undesired transition from an operating condition to another could be eliminated in the system design stage. Besides, there are in the literature some evidences of connections between input multiplicity and right-half plane zeros [13]. It is important to stress that the presence of right-half plane zeros limit the achievable closed-loop performance, regardless of the control law used. Output multiplicities also might have an adverse effect on feedback control performance. This type of multiplicities arise when for the same value of an input variable different responses, of a variable chosen as system output, are obtained. In this work two other kinds of nonlinearities are analyzed: isolas and disjoint bifurcations. Isolas correspond to isolated loops of steady-state solutions [7]. Disjoint bifurcations are branches of disconnected steady-state solutions which emerge when the parameter selected as the continuation parameter takes physical limit values [5]. Fig. 9 in [10] shows the typical shape of regions of disjoint bifurcations.

Applying singularity theory, Farr and Aris [4] found up to five steady-states for the series reaction. As consequence the series reaction might display more complex bifurcation maps than those exhibited by the single reaction A→ B which shows up to three steady-states. Most of the published works on the nonlinear behaviour of CSTRs where the reactions A→ B → C take place do not take into account

* Corresponding author. Tel.: +52-5-267-42-79; fax: +52-5-267-42-79.
E-mail address: antonio.flores@uia.mx (A. Flores-Tlacuahuac).

1385-8947/00/$ – see front matter
PII: S1385-8947(99)00157-6

the jacket energy balance [2,3,6]. Only recently Russo and Bequette [10] had shown the impact, on the operability of a CSTR where the reaction A→ B takes place, of including the jacket energy balance when modeling CSTR's. These authors had shown that adding the jacket energy balance to the modeling phase of chemical reactors have a deep impact on the open-loop nonlinear behaviour. Recently Russo and Bequette [11] conducted a bifurcation analysis on a free-radical styrene polymerization reactor. Although the kinetic model becomes more complicated the conclusions reached were similar to those found previously by the same authors in reactors with simpler kinetic models [10]. They also used perturbation theory to analyze the way process design changes affect the amplitude of oscillations when the reactor happens to operate in a Hopf bifurcation point. In this paper the work done by Russo and Bequette [10] for a single irreversible chemical reaction is extended to the case of two irreversible first order reactions. Most of the basic conclusions related to this topic were first found by Russo and Bequette [10], however the case treated in this paper was not considered by those authors.

The contents of this paper are next outlined. In Section 2 a description of the mathematical model and the dimensionless process are shown. In Section 3 theoretical conditions for the emergence of nonlinear behaviour are mentioned. In this section the multiplicity analysis is performed for both the short and full models. In Section 4 the multiplicity results for both kinds of models are discussed. In Section 5 the nonlinear behaviour obtained for the two modeling approaches, using the same set of process parameters, is compared. Finally in Section 6 the main conclusions of this paper are stressed.

2. Process modeling

The mathematical model which describes a CSTR in which two exothermic irreversible first-order reactions in series A→ B → C take place is derived from dynamic material and energy balances. Reactor volume and physical parameters are assumed to remain constant; perfect mixing is also assumed. In addition the dynamics of the cooling jacket is taken into account. The model consists of the following four nonlinear ordinary differential equations:

$$\frac{dC_A}{dt} = \frac{Q}{V}(C_{Af} - C_A) - k_1(T)C_A \tag{1}$$

$$\frac{dC_B}{dt} = \frac{Q}{V}(C_{Bf} - C_B) - k_2(T)C_B + k_1(T)C_A \tag{2}$$

$$\frac{dT}{dt} = \frac{Q}{V}(T_f - T) + k_1(T)C_A\frac{(-\Delta H_A)}{\rho C_p} + k_2(T)C_B\frac{(-\Delta H_B)}{\rho C_p} - \frac{UA}{\rho C_p V}(T - T_c) \tag{3}$$

$$\frac{dT_c}{dt} = \frac{Q_c}{V_c}(T_{cf} - T_c) + \frac{UA}{\rho_c C_{pc} V_c}(T - T_c) \tag{4}$$

where the kinetic constants are:

$$k_1(T) = A_1 e^{-E_1/RT} \tag{5}$$

$$k_2(T) = A_2 e^{-E_2/RT} \tag{6}$$

Eqs. (1)–(4) to can be written in dimensionless form as:

$$\frac{dx_1}{d\tau} = q(x_{1f} - x_1) - x_1\eta(x_3)\phi \tag{7}$$

$$\frac{dx_2}{d\tau} = q(x_{2f} - x_2) - x_2\phi S\eta_2(x_3) + x_1\phi\eta(x_3) \tag{8}$$

$$\frac{dx_3}{d\tau} = q(x_{3f} - x_3) + \delta(x_4 - x_3) + \beta\phi[x_1\eta(x_3) + \alpha x_2\eta_2(x_3)S] \tag{9}$$

$$\frac{dx_4}{d\tau} = \delta_1(q_c(x_{4f} - x_4) + \delta\delta_2(x_3 - x_4)) \tag{10}$$

where x_1 is the dimensionless concentration of reactant A, x_2 is the dimensionless concentration of reactant B, x_3 is the dimensionless reactor temperature and x_4 is the dimensionless cooling jacket temperature. Other dimensionless parameters are defined in Table 1. In this work the phrase *short model* stands for the CSTR mathematical model without including the jacket energy balance (Eqs. (1)–(3)), while the term *full model* will refer to the CSTR model including the jacket energy balance (Eqs. (1)–(4)).

3. Steady state multiplicity

In this section theoretical conditions for the existence of a class of nonlinear behaviour are addressed. Suppose a given function:

$$g(x, u) = 0 \tag{11}$$

Table 1
Dimensionless parameters

$x_1 = C_A/C_{Afo}$	$x_3 = ((T - T_{fo})/(T_{fo}))\gamma$	$x_4 = ((T_c - T_{fo})/(T_{fo}))\gamma$	$x_2 = C_B/C_{Afo}$
$\gamma = E_1/RT_{fo}$	$\psi = E_2/E_1$	$\tau = (Q_o/V)t$	$q = Q/Q_o$
$q_c = Q_c/Q_o$	$\delta = UA/\rho C_p Q_o$	$\delta_1 = V/V_c$	$\delta_2 = \rho C_p/\rho_c C_{pc}$
$S = (k_2(T_{fo}))/(k_1(T_{fo}))$	$\phi = (V/Q_o)k_1(T_{fo})$	$\beta = -\Delta H_a C_{Afo}\gamma/\rho C p T_{fo}$	$\alpha = -\Delta H_b/-\Delta H_a$
$x_{1f} = C_{Af}/C_{Afo}$	$x_{3f} = ((T_f - T_{fo})/(T_{fo}))\gamma$	$x_{4f} = ((T_{cf} - T_{fo})/T_{fo}))\gamma$	$x_{2f} = C_{Bf}/C_{Afo}$
$\eta(x_3) = \exp[x_3/(1 + (x_3/\gamma))]$	$\eta_2(x_3) = \exp[x_3/(1 + (x_3/\gamma))]$		

where u stands for an input parameter and x stands for an output parameter (or system state). Then from the implicit function theorem the necessary conditions for the existence of output multiplicity, input multiplicity, and isolas are given by:

$$g = \frac{\partial g}{\partial x} = 0 \tag{12}$$

$$g = \frac{\partial g}{\partial u} = 0 \tag{13}$$

$$g = \frac{\partial g}{\partial x} = \frac{\partial g}{\partial u} = 0 \tag{14}$$

respectively. The number of output multiplicities can be evaluated from catastrophe theory [9]. If:

$$g = \frac{\partial g}{\partial x} = \frac{\partial^2 g}{\partial x^2} = \cdots = \frac{\partial^n g}{\partial x^n} = 0 \tag{15}$$

and

$$\frac{\partial^{n+1} g}{\partial x^{n+1}} \neq 0 \tag{16}$$

then $n+1$ output multiplicities will exist around the codimension n singular point x which is a solution of Eq. (15). Next, in order to detect input/output multiplicity and isolas formation, the theoretical conditions mentioned in this part are applied to both the short and full models.

3.1. Short model

In order to detect potential nonlinear behaviour the dimensionless model must be combined into a single algebraic equation. Under steady-state conditions Eqs. (7) and (8) can be solved for x_1 and x_2, respectively. If these equations are substituted into Eq. (9) then the following single algebraic equation will be obtained:

$$g(x_3) = q(x_{3\mathrm{f}} - x_3) + \delta(x_4 - x_3) + \beta\phi\left[\frac{q x_{1\mathrm{f}}\eta}{q+\eta\phi} + \frac{\alpha\eta S q}{q+\eta_2 S\phi}\left(\frac{x_{1\mathrm{f}}\eta\phi}{q+\eta\phi} + x_{2\mathrm{f}}\right)\right] \tag{17}$$

3.1.1. Output multiplicities

In order to analyze the presence of output multiplicities the first and second derivatives of g with respect to x_3 are obtained (due to the complexity of the analytical derivatives only first and second derivatives were examined). All the derivatives were evaluated using the symbolic manipulation facilities available in the Matlab Symbolic Math toolbox [14].

$$\frac{\partial g}{\partial x_3} = -q - \delta + \frac{\beta\phi q x_{1\mathrm{f}} C\eta E}{I} - \frac{\beta\phi^2 q x_{1\mathrm{f}}\eta^2 E C}{I^2} + \frac{\beta\phi q x_{1\mathrm{f}}\eta}{I}\left[\frac{\alpha S\phi\eta C}{K} - \frac{\alpha S^2\phi^2\eta\psi C\eta_2}{K^2}\right] + \frac{\beta\phi\alpha S q x_{2\mathrm{f}} C\eta}{K} - \frac{\beta\phi^2\alpha S^2 q x_{2\mathrm{f}}\eta\psi C\eta_2}{K^2} \tag{18}$$

$$\begin{aligned}\frac{\partial^2 g}{\partial x_3^2} = {} & \frac{\beta\phi q x_{1\mathrm{f}} A\eta E}{I} + \frac{\beta\phi q x_{1\mathrm{f}} C^2\eta E}{I} - 3\frac{\beta\phi^2 q x_{1\mathrm{f}} C^2\eta^2 E}{I^2} \\ & + 2\frac{\beta\phi q x_{1\mathrm{f}} C\eta}{I}\left[\frac{\alpha S\phi C\eta}{K} - \frac{\alpha S^2\phi^2\eta\psi C\eta_2}{K^2}\right] \\ & + 2\frac{\beta\phi^3 q x_{1\mathrm{f}}\eta^3 E C^2}{I^3} - 2\frac{\beta\phi^2 q x_{1\mathrm{f}}\eta^2 C}{I^2}\left[\frac{\alpha S\phi C\eta}{K} - \frac{\alpha S^2\phi^2\eta\psi C\eta_2}{K^2}\right] - \frac{\beta\phi^2 q x_{1\mathrm{f}}\eta^2 E A}{I^2} \\ & + \frac{\beta\phi q x_{1\mathrm{f}}\eta}{I}\left(\frac{\alpha S\phi A\eta}{K} + \frac{\alpha S\phi C^2\eta}{K} - \frac{2\alpha S^2\phi^2 C^2\eta\psi\eta_2}{K^2} + \frac{2\alpha S^3\phi^3\eta(\psi C)^2\eta_2^2}{K^3} - \frac{\alpha S^2\phi^2\eta\psi A\eta_2}{K^2} - \frac{\alpha S^2\phi^2\eta\eta_2(\psi C)^2}{K^2}\right) \\ & + \frac{\beta\phi\alpha S q x_{2\mathrm{f}}\eta}{K}\left(A + C^2 - \frac{2\phi S\psi C^2\eta_2}{K} + \frac{2\phi^2 S^2(\psi C)^2\eta_2^2}{K^2} - \frac{\phi S A\psi\eta_2}{K} - \frac{\phi S(\psi C)^2\eta_2}{K}\right)\end{aligned} \tag{19}$$

where A, C, E, K and I are defined as follows:

$$A = \frac{-2}{\gamma(1+(x_3/\gamma))^2} + \frac{2x_3}{\gamma^2(1+(x_3/\gamma))^3} \tag{20}$$

$$C = \frac{1}{1+(x_3/\gamma)} - \frac{x_3}{\gamma(1+(x_3/\gamma))^2} \tag{21}$$

$$E = 1 + \frac{\alpha S\phi\eta}{K} \tag{22}$$

$$K = q + \eta_2 S\phi \tag{23}$$

$$I = q + \eta\phi \tag{24}$$

Under some conditions these two derivatives could be equal to zero. The conditions to be fulfilled to guarantee the existence of three steady-states are given by:

$$g = \frac{\partial g}{\partial x_3} = \frac{\partial^2 g}{\partial x_3^2} = 0 \tag{25}$$

and

$$\frac{\partial^3 g}{\partial x^3} \neq 0 \tag{26}$$

3.1.2. Input multiplicities

According to the implicit function theorem to guarantee the presence of input multiplicities the following condition must be met:

$$g(x,\lambda) = \frac{\partial g(x,\lambda)}{\partial\lambda} = 0 \tag{27}$$

where λ are the system parameters with respect to which the existence of input multiplicities is suspected, in our case: $\lambda = [x_{1\mathrm{f}}, x_{3\mathrm{f}}, x_4, q]$. Next the analysis to check whether or not the system exhibits input multiplicities is performed.

- x_{1f}

$$\frac{\partial g}{\partial x_{1f}} = \frac{\beta\phi q\eta}{q+\eta\phi}\left(1+\frac{\phi\alpha\eta S}{q+\eta_2 S\phi}\right) \tag{28}$$

In this case taking into account the numerical values that the parameters could assume the above equation cannot be equal to zero. Therefore no input multiplicities with respect to the feedstream concentration can exist.

- x_{3f}

$$\frac{\partial g}{\partial x_{3f}} = q \tag{29}$$

This equation cannot be equal to zero, unless no reactants are fed to the reactor. This is an impractical situation. Hence no input multiplicities with respect to the feedstream temperature are possible.

- x_4

$$\frac{\partial g}{\partial x_4} = \delta \tag{30}$$

There are no input multiplicities since the parameter δ cannot be equal to zero, unless the heat transfer coefficient or the heat transfer area are equal to zero which is an infeasible situation.

- q

$$\frac{\partial g}{\partial q} = (x_{3f}-x_3)+\beta\phi\left[\frac{x_{1f}\eta}{I}-\frac{qx_{1f}\eta}{I^2}+\frac{\alpha\eta\beta S}{q+\eta_2\phi S} -\frac{\alpha\eta\beta Sq}{(q+\eta_2\phi S)^2}-\frac{\alpha\eta^2 Sq}{q+\eta_2 S\phi}\left(\frac{x_{1f}\phi}{I^2}\right)\right] \tag{31}$$

The situation might be different in this case. Under certain combinations of the value of some parameters the above first derivative could be equal to zero. Therefore input multiplicities with respect to the volumetric feedrate might exist.

3.1.3. Isolas

If a given system presents both input and output multiplicities, which means it satisfies the equations:

$$g(x,\lambda) = \frac{\partial g}{\partial x} = \frac{\partial g}{\partial \lambda} = 0 \tag{32}$$

then it might give rise to isola behaviour which corresponds to isolated operating regions. In our case λ is the dimensionless volumetric flowrate q and x corresponds to x_3 since it is the state which respect to which output multiplicities are present. Hence in order to guarantee the presence of isola behaviour the following condition must be met:

$$g(x_3,q) = \frac{\partial g}{\partial x_3} = \frac{\partial g}{\partial q} = 0 \tag{33}$$

3.2. Full model

In order to find input/output multiplicity the dimensionless model must be combined into a single algebraic equation. Under steady-state conditions Eqs. (7), (8) and (10) can be solved for x_1, x_2 and x_4, respectively. If these equations are substituted into Eq. (9) then the following algebraic equation will be obtained:

$$h(x_3,q_c,\boldsymbol{p}) = q(x_{3f}-x_3)+\delta\left(\frac{\delta\delta_2 x_3+q_c x_{4f}}{q_c+\delta\delta_2}-x_3\right) +\beta\phi\left[\frac{qx_{1f}\eta}{q+\eta\phi}+\frac{\alpha\eta Sq}{q+\eta_2 S\phi}\left(\frac{x_{1f}\eta\phi}{q+\eta\phi}+x_{2f}\right)\right] \tag{34}$$

where x_3 is the controlled output, q_c is the manipulated input and $\boldsymbol{p}$ is the vector containing the system parameters. This equation is used to perform the multiplicity analysis.

3.2.1. Output multiplicities

In order to find output multiplicities the implicit function theorem is applied again. The first and second derivatives of the single combined nonlinear equation h with respect to x_3 are obtained (again due to the complexity of the analytical derivatives only first and second derivatives were examined).

$$\frac{\partial h}{\partial x_3} = -q+\delta\left(\frac{\delta\delta_2}{q_c+\delta\delta_2}-1\right)+\frac{\beta\phi q x_{1f}C\eta E}{I} -\frac{\beta\phi^2 q x_{1f}\eta^2 EC}{I^2}+\frac{\beta\phi q x_{1f}\eta}{I}\left[\frac{\alpha S\phi\eta C}{K} -\frac{\alpha S^2\phi^2\eta\psi C\eta_2}{K^2}\right]+\frac{\beta\phi\alpha Sq x_{2f}C\eta}{K} -\frac{\beta\phi^2\alpha S^2 q x_{2f}\eta\psi C\eta_2}{K^2} \tag{35}$$

$$\frac{\partial^2 h}{\partial x_3^2} = \frac{\beta\phi q x_{1f}A\eta E}{I}+\frac{\beta\phi q x_{1f}C^2\eta E}{I}-3\frac{\beta\phi^2 q x_{1f}C^2\eta^2 E}{I^2} +2\frac{\beta\phi q x_{1f}C\eta}{I}\left[\frac{\alpha S\phi C\eta}{K}-\frac{\alpha S^2\phi^2\eta\psi C\eta_2}{K^2}\right] +2\frac{\beta\phi^3 q x_{1f}\eta^3 EC^2}{I^3}-2\frac{\beta\phi^2 q x_{1f}\eta^2 C}{I^2}\left[\frac{\alpha S\phi C\eta}{K} -\frac{\alpha S^2\phi^2\eta\psi C\eta_2}{K^2}\right]-\frac{\beta\phi^2 q x_{1f}\eta^2 EA}{I^2}+\frac{\beta\phi q x_{1f}\eta}{I} \times\left(\frac{\alpha S\phi A\eta}{K}+\frac{\alpha S\phi C^2\eta}{K}-\frac{2\alpha S^2\phi^2 C^2\eta\psi\eta_2}{K^2} +\frac{2\alpha S^3\phi^3\eta(\psi C)^2\eta_2^2}{K^3}-\frac{\alpha S^2\phi^2\eta\psi A\eta_2}{K^2} -\frac{\alpha S^2\phi^2\eta\eta_2(\psi C)^2}{K^2}\right)+\frac{\beta\phi\alpha Sq x_{2f}\eta}{K}\left(A+C^2 -\frac{2\phi S\psi C^2\eta_2}{K}+\frac{2\phi^2 S^2(\psi C)^2\eta_2^2}{K^2}-\frac{\phi SA\psi\eta_2}{K} -\frac{\phi S(\psi C)^2\eta_2}{K}\right) \tag{36}$$

where A, C, E, K and I are given by Eqs. (20)–(24). Output multiplicities with respect to x_3 are possible since, under

combination of certain values of the parameters, the next set of equations might be met:

$$h = \frac{\partial h}{\partial x_3} = \frac{\partial^2 h}{\partial x_3^2} = 0 \tag{37}$$

and

$$\frac{\partial^3 h}{\partial x_3^3} \neq 0 \tag{38}$$

3.2.2. Input multiplicities

In order to guarantee the presence of input multiplicities with respect to the vector of paramerers λ, Eq. (27) should be satisfied. λ will be given by: $[x_{1f}, x_{3f}, x_{4f}, q, q_c]$. Next we perform the input multiplicity analysis.

- x_{1f}

$$\frac{\partial h}{\partial x_{1f}} = \frac{\beta\phi q\eta}{q+\eta\phi}\left(1 + \frac{\phi\alpha\eta S}{q+\eta_2 S\phi}\right) \tag{39}$$

With the allowed numerical values of the parameters no input multiplicities exist with respect to the feedstream concentration of reactant A.

- x_{3f}

$$\frac{\partial h}{\partial x_{3f}} = q \tag{40}$$

This equation is equal to zero only when there is not volumetric flowrate which is not a feasible condition. So no input multiplicities exist with respect to the temperature feedstream.

- x_{4f}

$$\frac{\partial h}{\partial x_{4f}} = \frac{\delta q_c}{q_c + \delta\delta_2} \tag{41}$$

Since the cooling water flowrate, the heat transfer coefficient or the heat transfer area cannot be equal to zero, no input multiplicities exist with respect to the dimensionless cooling water temperature .

- q_c

$$\frac{\partial h}{\partial q_c} = \frac{\delta x_{4f}}{q_c + \delta\delta_2} - \frac{\delta(\delta\delta_2 x_3 + q_c x_{4f})}{(q_c + \delta\delta_2)^2} \tag{42}$$

With an appropriate combination of the numerical values of the parameters, input multiplicities with respect to the dimensionless cooling water volumetric flowrate might exist.

- q

$$\frac{\partial h}{\partial q} = (x_{3f} - x_3) + \beta\phi\left[\frac{x_{1f}\eta}{I} - \frac{q x_{1f}\eta}{I^2} + \frac{\alpha\eta S B}{q+\eta_2 S\phi} - \frac{\alpha\eta S q B}{(q+\eta_2 S\phi)^2} - \frac{\alpha\eta^2 S q}{q+\eta_2 S\phi}\left(\frac{x_{1f}\phi}{I^2}\right)\right] \tag{43}$$

In this case input multiplicities with respect to the volumetric flowrate might exist since, with the appropriate combination of the numerical values of the parameters, the above equation could be satisfied.

3.2.3. Isolas

As we said before, in order to get isola behaviour the following equation must be satisfied:

$$h(x, \lambda) = \frac{\partial h}{\partial x} = \frac{\partial h}{\partial \lambda} = 0 \tag{44}$$

for the full model $\lambda = q_c$ and $x = x_3$.

4. Nonlinear analysis results

In this section we show nonlinear behaviour results obtained for the short and full models. All the bifurcation diagrams were obtained using the XPP-AUTO software [12].

4.1. Short model

4.1.1. Input multiplicities

From the analysis of Section 3.1 input multiplicities are only possible when the volumetric flowrate q is the input or manipulated variable. Therefore input multiplicities only were looked for with respect to this parameter. For the short model two different q values resulted in the same reactor temperature (Fig. 1). The parameters used in this part are shown in Table 2. The steady-state multiplicity region can be decreased or increased by changing the δ parameter, this parameter is related to the heat transfer area. When δ is small (δ=0.5) the multiplicity region is wide and a maximum is present. Increasing δ up to 3 the maximum disappears and a unique region is observed. A reactor operating around this last region could be safe to operate because changes in the volumetric feedflowrate lead to small variations in the reactor temperature. Quite the contrary similar changes in the former region could lead to operational problems.

Changing the exothermicity of the first reaction the reactor temperature response is modified (Fig. 2). Since the ratio

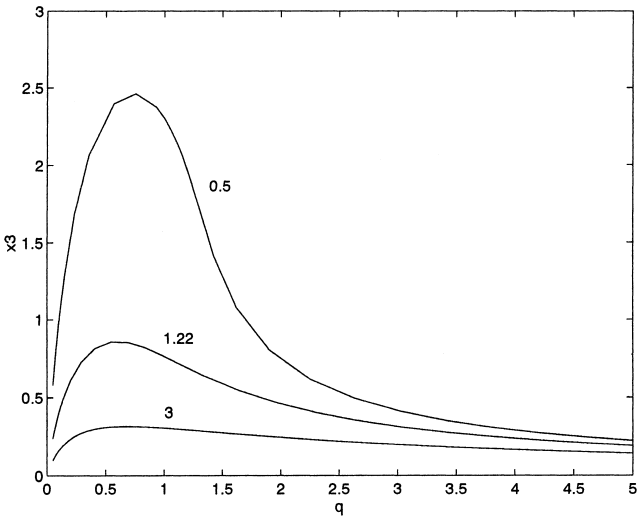

Fig. 1. Short model input multiplicity changing δ.

Table 2
Parameters for input multiplicity using the short model

Figure	β	ϕ	δ	α	S	ψ	γ	x_{1f}	x_{2f}	x_{3f}	x_{4f}
1	4.9	0.28	···	1.11	0.94	0.35	22.7	0.73	0	0	0
2	···	0.28	1.22	1.11	0.94	0.35	22.7	0.73	0	0	0
3	3	1.47	···	1.11	1.79	0.89	13	1	0	0.28	0.53

of reaction heats is kept constant ($\alpha = 1.11$) changes in the β parameter mean that the two reactions become more exothermic simultaneously. By increasing the exothermicity of both reactions the input multiplicity region, between q and x_3, will be wider.

In Fig. 3 input and output multiplicities are shown for different δ values. δ might be modified changing the heat transfer area. A region of hysteresis behaviour is also shown (denoted by dotted lines). In this region the reactor temperature *jumps* from the high temperature stable steady-state to the low temperature stable steady-state. The main differences between Figs. 3 and 1 are that the second reaction is faster ($S > 1$) than the first one, and that the reactant is more concentrated ($x_{1f} = 1$) and preheated ($x_{3f} = 0.28$). Besides increasing the heat transfer area (δ) leads to remove the output multiplicities.

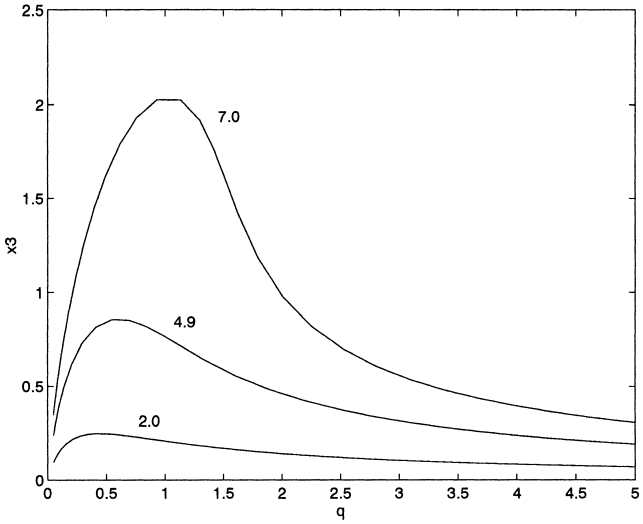

Fig. 2. Short model input multiplicity changing β.

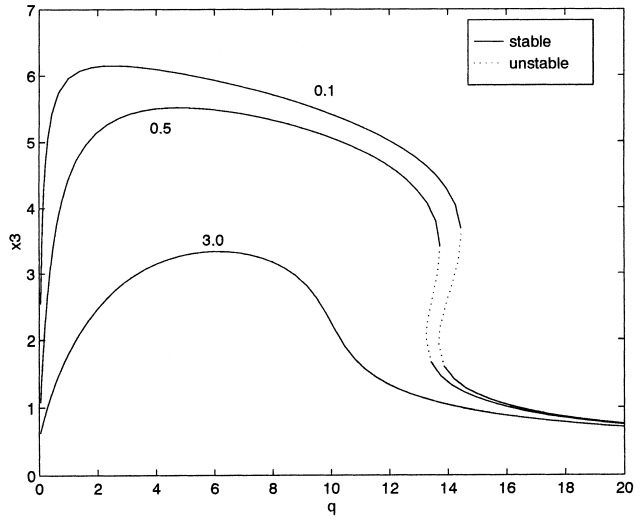

Fig. 3. Short model output and input multiplicity changing δ.

4.1.2. Output multiplicities

In this section we analyze the effect of the feedflowrate and the cooling water temperature on the output multiplicity behaviour. These two variables were selected because the implicit function theorem showed that input multiplicities are only possible when the feedflowrate is taken as the input parameter (besides if output multiplicities are present as well, isola behaviour could be observed too), and because we decided to address the effect of including the energy balance in the modeling process.

Using the dimensionless feedflowrate q as continuation parameter, and the dimensionless parameters shown in Table 3, several kinds of behaviours were observed. Input and output multiplicities are present (Fig. 4). This means that isolated operating regions should also be observed. Besides, ignition (1.34, 1.17), (2.57, 1.31) and extinction (5.39, 6.15), (7.8, 6.87) points are also present. The appearance of the isola operating region, as function of the δ parameter, is also shown in Fig. 4. Increasing q, keeping δ constant, a unique region is obtained; in this region the reactor temperature is smaller than the reference temperature T_{fo}.

The effect of changing the reaction exothermicity was also analyzed (Fig. 5). The ratio of the heats of reaction was kept constant ($\alpha = 1.18$). However we also considered the case when the second reaction becomes more exothermic than the first one ($\alpha > 1$). In this situation, and using the parameters from Table 3, isola formation was not observed; however input and output multiplicities were present. Such behaviour could be explained noting that the reactor is not overcooled. According to Hlavacek and Van Rompay [7] isola behaviour is generally observed in overcooled systems. In the past case the dimensionless cooling water temperature was $x_{4f} = -0.82$ while in this case $x_{4f} = 0$. Output multiplicities give rise to ignition (2.13, 2.06), (3.22, 1.99), (4.26, 1.94) and extinction points (2.47, 3.91), (6.51, 5.9), (13.84, 7.33).

Input and output multiplicities were also observed for changes in the Damkhöler number (Fig. 6). By decreasing the Damkhöler number an isola region appears. However with $\phi = 0.058$ a branch of low and high temperature is

Table 3
Parameters for output multiplicity using the short model

Figure	β	ϕ	δ	q	α	S	ψ	γ	x_{1f}	x_{2f}	x_{3f}	x_{4f}
4	8.01	0.16	···	C	0.92	0.84	0.41	19.42	1.06	0	0.13	−0.82
5	···	0.17	0.73	C	1.18	1.02	0.34	25.54	0.28	0	0.5	0
6	30	···	0.73	C	1.18	1.02	0.34	25.54	0.28	0	0.5	0
7	8.01	0.07	0.3	1	0.92	0.84	0.41	19.42	1.06	0	0.13	C

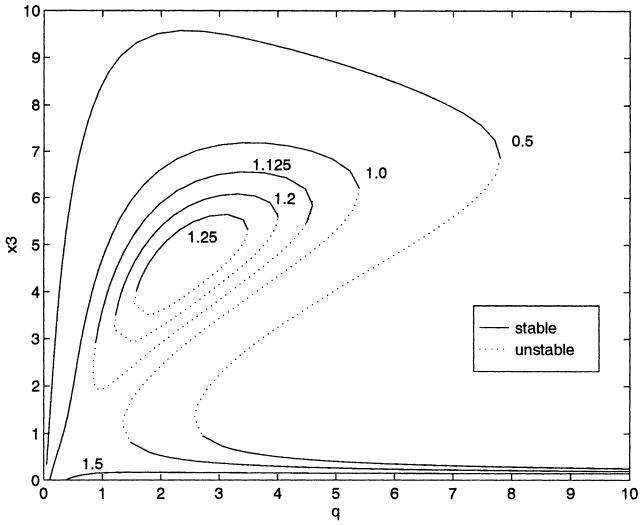

Fig. 4. Short model input, output multiplicity and isola formation changing δ.

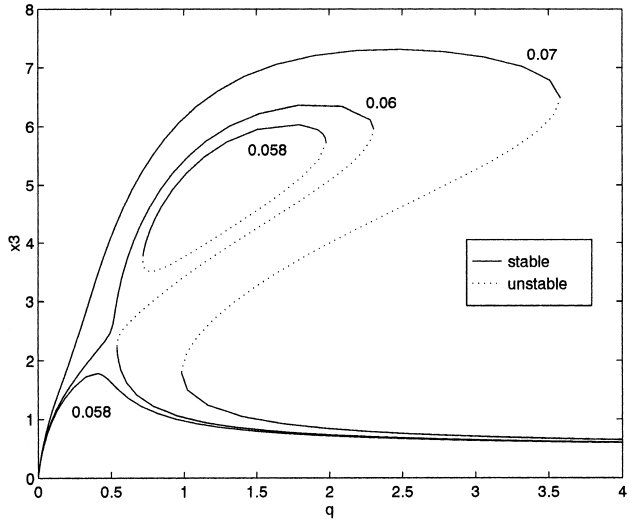

Fig. 6. Short model input, output multiplicity and isola formation changing ϕ.

observed. Isola behaviour is only present for the high temperature region.

Finally output multiplicities with respect to the dimensionless cooling water temperature were analyzed. Fig. 7 shows the existence of output multiplicities. In practical situations the cooling water temperature is seldom constant due to the heat transfer characteristics of the process. Constant cooling temperatures might be obtained using a boiling liquid (an usually impractical situation). In terms of process control this means that the cooling temperature is not a good manipulated variable. However, for control purposes the cooling water flowrate is much easier to handle. Therefore, during the reactor modeling phase the cooling medium dynamics should be included.

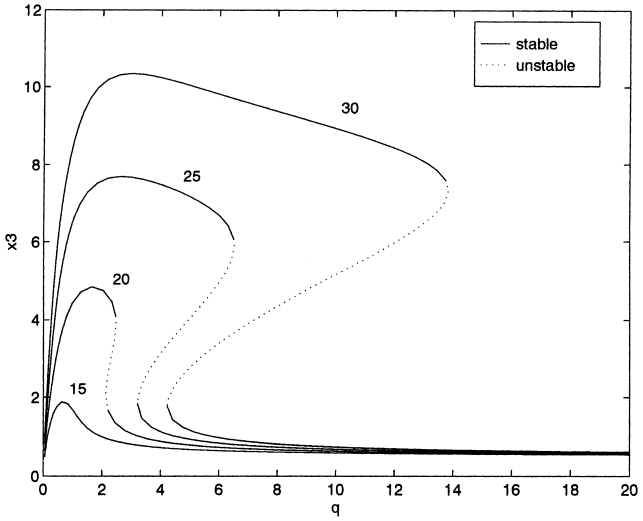

Fig. 5. Short model input, output multiplicity changing β.

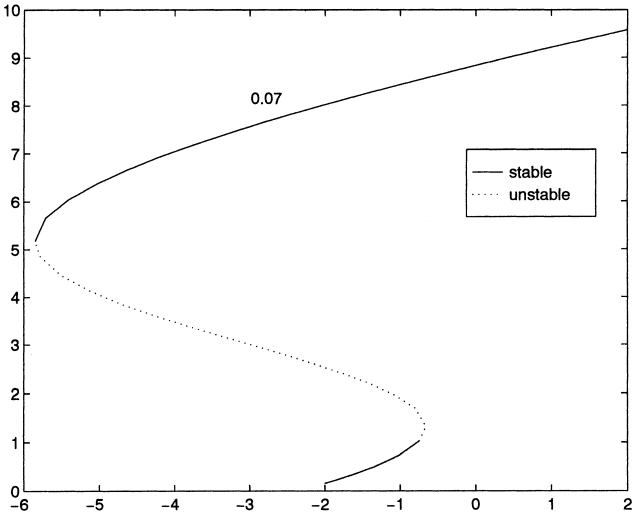

Fig. 7. Short model output multiplicities using $\phi = 0.07$.

4.2. Full model

In order to analyze input/output multiplicities, using the full order model, the dimensionless cooling water flowrate q_c was used as continuation parameter. We have selected this parameter since it is easy to manipulate and in addition output multiplicities with respect to the dimensionless cooling water temperature, using the reduced model, were observed.

In the bifurcation diagrams, obtained plotting x_3 versus q_c, up to five different operating regions can be observed. Region I is a unique region (Fig. 8), while region II (Fig. 9) is the traditional s-shaped curve denoting ignition and extinction behaviour.

The presence of constraints (natural or forced) on the value of the manipulated variables is a well known source of infeasible operating regions [10]. For instance, in the limit when $q_c \to 0$, infeasible operating regions, known as

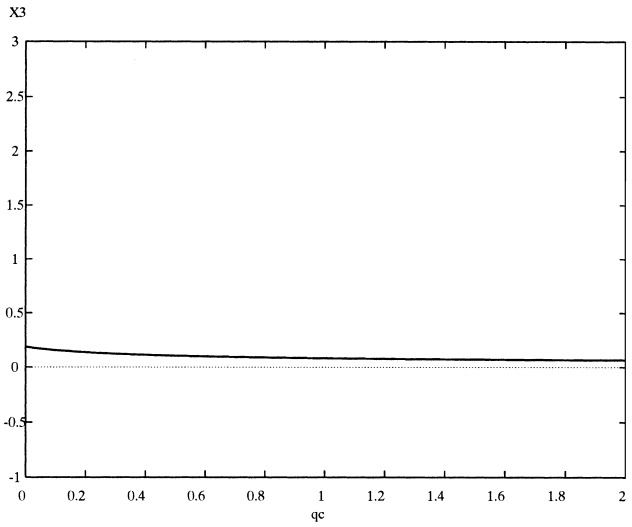

Fig. 8. Full model, region I using $\beta = 8$, $\phi = 0.02$.

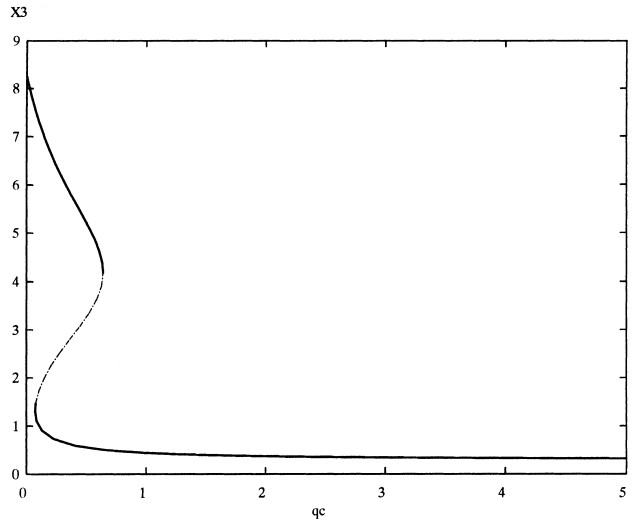

Fig. 9. Full model, region II using $\beta = 8$, $\phi = 0.06$.

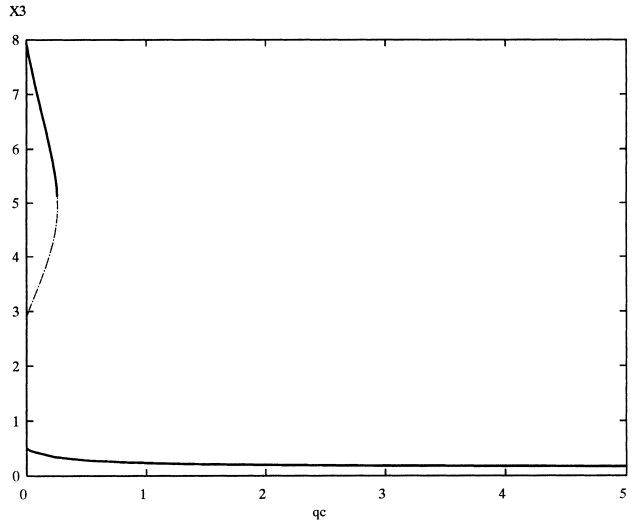

Fig. 10. Full model, region III using $\beta = 8$, $\phi = 0.04$.

"0-disjoint" regions, appear. This sort of regions corresponds to infeasible low temperature operating regions. Such bifurcations are shown as regions III (Fig. 10). When $q_c \to \infty$ another sort of infeasible operating regions, known as "∞-disjoint" bifurcations, are present. These sort of bifurcations give rise to operating regions denoted as regions IV (Fig. 11). They represent high temperature infeasible operating regions. The operating region V (Fig. 12) exhibits both sort of disjoint bifurcation behaviour. Parameters used for generating those diagrams are shown in Table 4.

The above five kinds of behaviour might show some variations if the parameter γ changes its value. This change

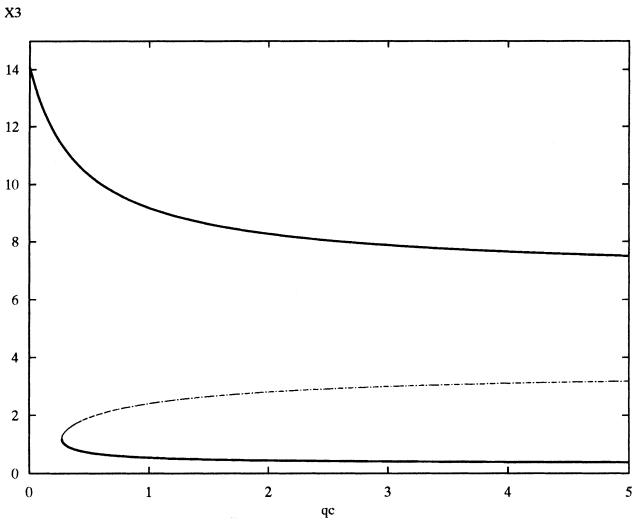

Fig. 11. Full model, region IV using $\beta = 13$, $\phi = 0.04$.

Table 4
Common parameters for the full model

δ	q	α	S	ψ	δ_1	δ_2	γ	x_{1f}	x_{2f}	x_{3f}	x_{4f}
0.78	1	0.19	1.015	0.32	10	0.952	27.85	1	0	0	−1

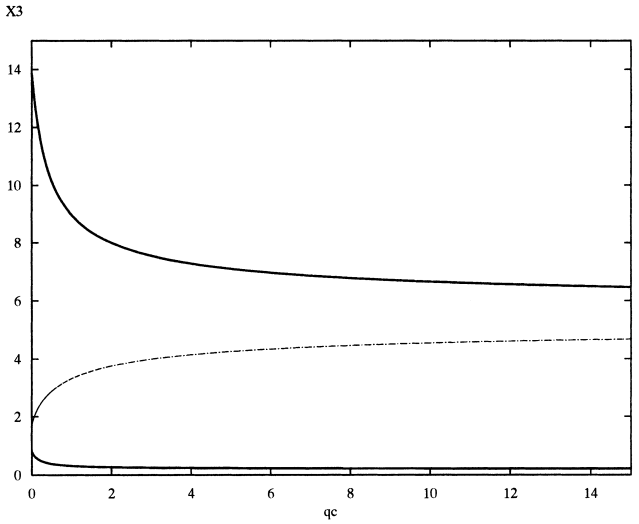

Fig. 12. Full model, region V using $\beta = 13$, $\phi = 0.03$.

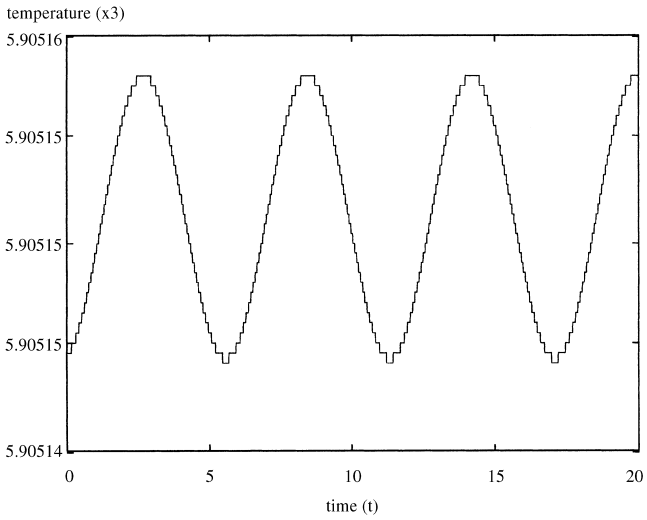

Fig. 14. Dynamic simulation starting from a Hopf bifurcation point.

could be equivalent to incorporating the exponential approximation in the modeling phase. For instance in the operating region II up to five steady-states were detected instead of three steady-states (Fig. 13). Besides Hopf bifurcations, corresponding to oscillatory solutions, are also shown in this figure. An open-loop dynamic simulation of the reactor, starting from a Hopf bifurcation point, is shown in Fig. 14 .

The operating region III also shows some variations. The "0-disjoint" region is present, but five steady-states were observed (Figs. 15 and 16). Some steady-states were open-loop unstable. Parameters used for these cases are shown in Table 5.

It is important to consider that although Byeon and Chung [2] reported a maximum of 7 steady-states for a CSTR with 2 reactions in series, they did not take into account the cooling water dynamics and they applied the exponential approximation. This questions the use of the exponential approxi-

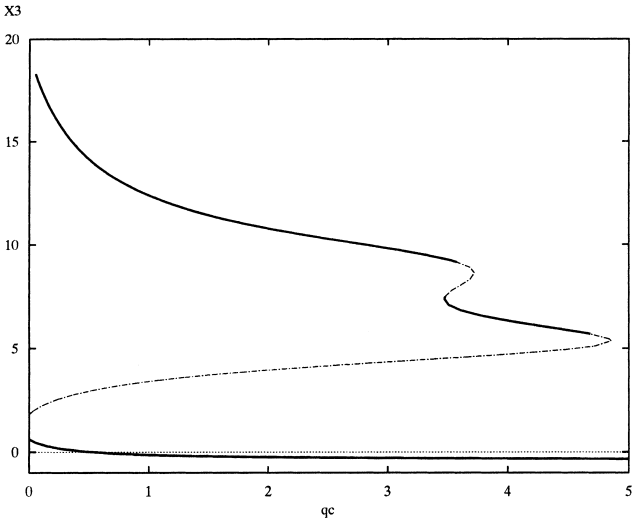

Fig. 15. Full model, variation of region III.

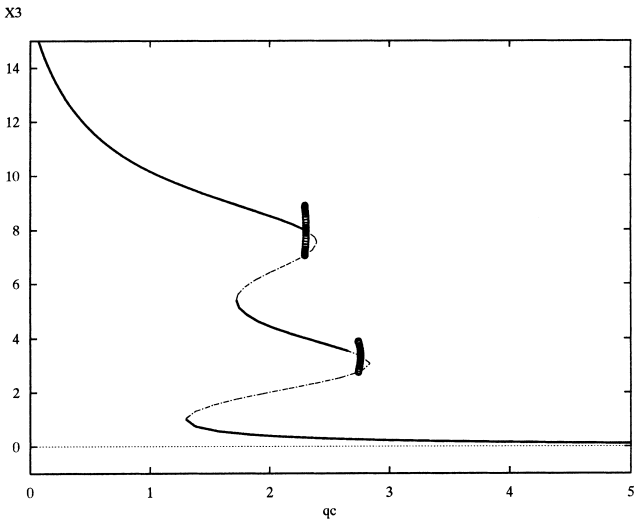

Fig. 13. Full model, region II with 2 Hopf bifurcation points.

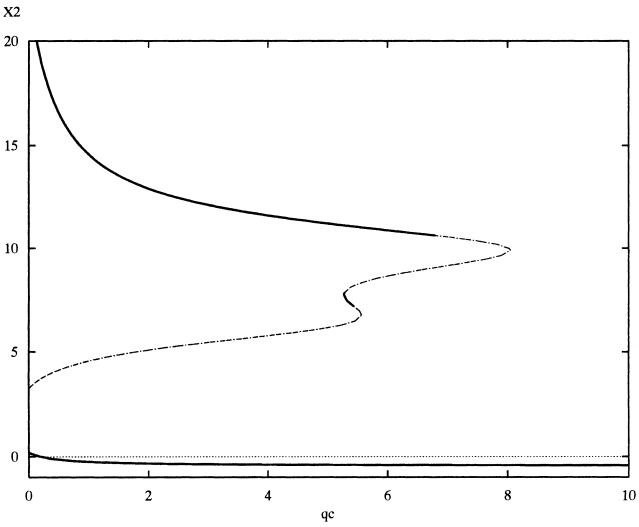

Fig. 16. Full model, variation of region III.

Table 5
Parameters for changes in the full model

Figure	β	ϕ	δ	q	α	S	ψ	δ_1	δ_2	γ	x_{1f}	x_{2f}	x_{3f}	x_{4f}
13	8	0.133	1	1	1	0.01	1	10	1	1000	1	0	0	−1
15	12	0.029	1	1	0.6	0.01	1	10	1	1000	1	0	0	−1
16	14	0.116	1	1	0.6	0.01	1	10	1	1000	1	0	0	−1

mation, since it may give rise to behaviour that cannot be observed if such approximation is not considered. In our study we have detected up to three steady-states using the full order model and without taking into account the exponential approximation. Five steady-states were only observed when the parameter γ was increased which it is equivalent to use the exponential approximation.

5. Discussion

In this section we discuss and compare the nonlinear behaviour implications of the short and full models using similar operation and design parameters.

Multiple steady-state behaviour changes if the cooling jacket energy balance is taken into account. For instance if the parameters shown in Table 4 are considered (setting $\beta = 8$ and $\phi = 0.06$) then using the short model no output multiplicity exists between the reactor temperature (x_3) and the cooling water temperature (x_4) (Fig. 17), while the full model exhibits output multiplicity between the reactor temperature and the cooling water flowrate (q_c) (Fig. 9). Those figures show that both the short and full models might exhibit completely different multiplicity behaviour for the same set of operation and design parameters.

In order to determine whether or not a given operating region is feasible, from an operation point of view, we should analyse if such region might contain disjoint branches of steady states when the manipulated variable tends to its boundary values. Those limit values give rise to disjoint bifurcartions. For the full model the manipulated variable is the cooling water flowrate (q_c) whose operational limits are $q_c = 0$ and $q_c = \infty$, this means that disjoint bifurcation regions were looked for inside this interval.

Using the parameters from Table 4, but changing $\beta = 8$ and $\phi = 0.04$, the short model does not exhibit output multiplicity behaviour (Fig. 18). However, using the full model, "0-disjoint" bifurcations can be observed (Fig. 10). When this sort of bifurcation emerges branches of separated steady-states are obtained for $q_c = 0$, and , as consequence, output multiplicity behaviour is also observed.

Again, if the same set of parameters is used, but changing $\beta = 13$ and $\phi = 0.04$, the short model exhibits output multiplicity behaviour (Fig. 19). However, using the the full model, "∞-disjoint" operating region (branches of separated steady-states obtained when $q_c = \infty$) are predicted (Fig. 11).

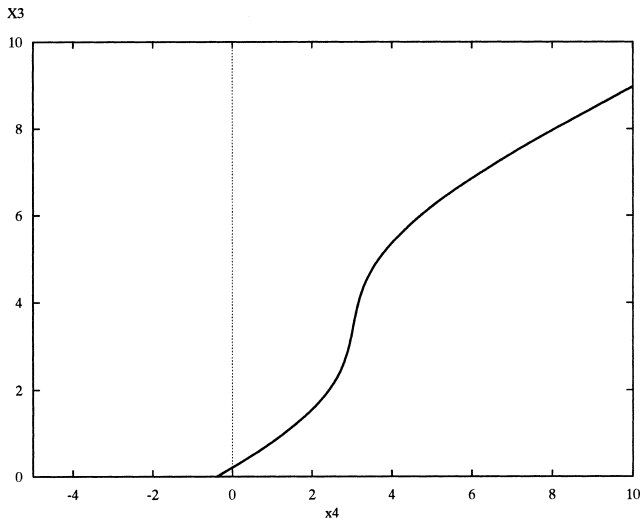

Fig. 18. Short model, region I setting $\beta = 8$, $\phi = 0.04$.

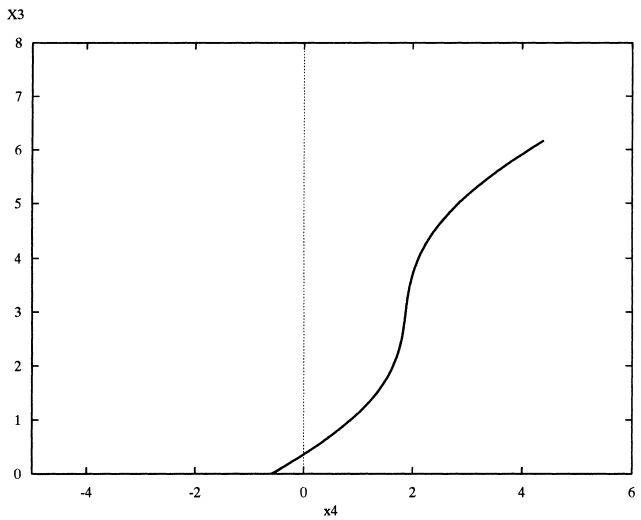

Fig. 17. Short model, region I setting $\beta = 8$, $\phi = 0.06$.

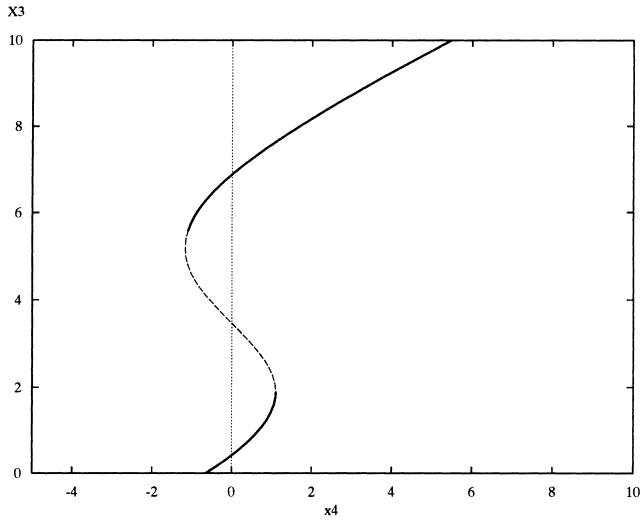

Fig. 19. Short model, region II setting $\beta = 13$, $\phi = 0.04$.

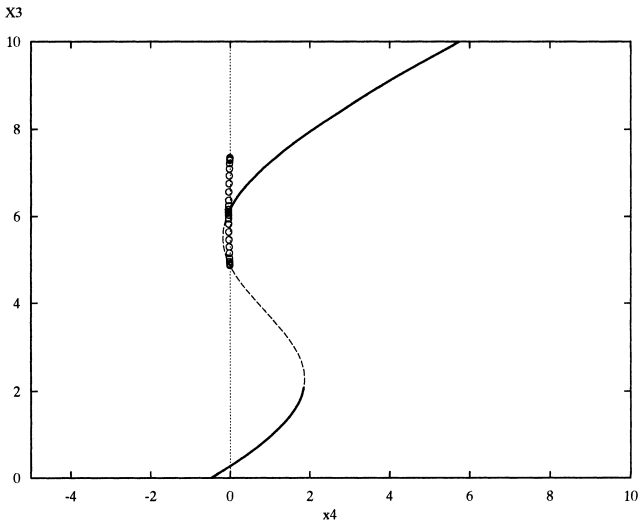

Fig. 20. Short model, region II with Hopf bifurcation points setting $\beta = 13$, $\phi = 0.03$.

Moreover the short model does not change its multiplicity behaviour if the Damkhöler number is changed to $\phi = 0.03$ (Fig. 20), however Hopf bifurcation points emerge. In this case the full model exhibits both an 0-disjoint and ∞-disjoint operating regions (Fig. 12).

All the above mentioned differences make it difficult to use the cooling water temperature as manipulated variable. However the cooling water flowrate is much easier to manipulate and in addition it may indicate if a given operating region is feasible from an operational point of view. The main conclusion of this part is that the full model should be used for control purposes.

6. Conclusions

In this paper we have shown that when modeling chemical reactors adding the cooling jacket energy balance may have a dramatic impact on the multiplicity behaviour. The full model may be open-loop unstable, due to the presence of output multiplicities, while the short model might be open-loop stable due to the fact that, using the same set of parameters, no output multiplicities are predicted.

Using the short model no input multiplicities and isolas were detected with respect to the reactor temperature. The same behaviour was observed for the full model with respect to the cooling water flowrate. Input multiplicities, which appear using the short model, between the reactor temperature and the feed flowrate, may be removed by increasing the heat transfer area and the heat transfer coefficient. Input multiplicity regions can be increased if the exothermicity of the reactions is raised. For the short model output multiplicities may be removed increasing the parameter δ. However care should be taken of the potential presence of isolas and a low temperature branch of steady-states using the same value of the mentioned parameter.

A conclusion from the work performed in this paper is that the more complicated series reaction is not generically so different from the simple case considered by Russo and Bequette [10]. The results reported in this paper could be interesting for people operating reactors where the series reactions take place. Using this knowledge a different operating point, where nonlinearities are not exhibited, could be chosen. From a control point of view, the results of this paper could provide more specific ideas about potential closed-loop problems in the form of input/output multiplicities and disjoint bifurcations.

7. Notation

A	Heat transfer area
A_1	Arrhenius preexponential factor (first reaction)
A_2	Arrhenius preexponential factor (second reaction)
C_A	Mol concentration reactant A
C_B	Mol concentration of component B
C_{Af}	Feedstream concentration of reactant A
C_{Bf}	Feedstream concentration of component B
C_p	Reaction mixture heat capacity
C_{pc}	Cooling medium heat capacity
E_1	Activation energy (first reaction)
E_2	Activation energy (second reaction)
k_1	Constant rate (first reaction)
k_2	Constant rate (second reaction)
Q	Volumetric feedflowrate
Q_c	Cooling medium volumetric flowrate
R	Ideal gas universal constant
t	Time
T	Reactor temperature
T_f	Feedstream temperature
T_{fo}	Reference temperature of the feedstream
T_c	Cooling medium temperature
T_{cf}	Cooling medium feedstream temperature
U	Heat transfer coefficient
V	Reactor volume
V_c	Cooling jacket volume
α	Heats of reaction ratio
β	Dimensionless heat of reaction A$\rightarrow$ B
ρ	Reaction mixture density
ρ_c	Cooling medium density
ΔH_a	Heat of reaction of the first reaction A$\rightarrow$ B
ΔH_b	Heat of reaction of the second reaction B$\rightarrow$ C

References

[1] R. Aris, Chemical reactors and some bifurcation phenomena, Ann. New York Acad. Sci. (1979) 314–331.

[2] K.H. Byeon, I.J. Chung, Analysis of the multiple Hopf bifurcation phenomena in a CSTR with two consecutive reactions — the singularity theory approach, Chem. Eng. Sci. 44(8) (1989) 1735–1742.

[3] E.J. Doedel, R.F. Heinemann, Numerical computation of periodic solution branches and oscillatory dynamics of the stirred tank reactor with A → B → C reactions, Chem. Eng. Sci. 38(9) (1983) 1493, 1499.
[4] W.W. Farr, R. Aris, Yet "Who Would have Thought the Old Man to Have so Much Blood in Him?" —Reflections on the multiplicity of steady-states of the stirred tank reactor, Chem. Eng. Sci. 41(6) (1986) 1385–1402.
[5] B.F. Gray, J.H. Merkin, G.C. Wake, Disjoint bifurcation diagrams in combustion systems, Math. Comp. Modelling 15 (1981) 25–33.
[6] D.C. Halbe, A.B. Poore, Dynamics of the continuous stirred tank reactor with reactions A→ B → C, Chem. Eng. J. 21 (1981) 241–253.
[7] V. Hlavacek, P. Van Rompay, On the birth and death of Isolas, Chem. Eng. Sci. 36(10) (1981) 1730–1731.
[8] L. Koppel, Input multiplicities in nonlinear multivariable control systems, AICHE. J. 28(6) (1982) 935–945.
[9] T. Poston, I. Stewart, Catastrophe Theory and Its Applications, Dover, 1978.
[10] L. Russo, W. Bequette, Impact of process design on the multiplicity behaviour of a jacketed exothermic CSTR, AICHE. J. 41(1) (1995) 135–147.
[11] L. Russo, W. Bequette, Operability of chemical reactors: multiplicity behavior of a jacketed styrene polymerization reactor, Chem. Eng. Sci. 53(1) (1998) 27–45.
[12] A. Silva, A. Flores, Nonlinear Analysis Using XPP, Proceedings of the DYCOPS-5 Conference, Corfu, Greece, June, 1998.
[13] P.B. Sistu, B.W. Bequette, Model Predictive Control of Process with Input Multiplicities, Chem. Eng. Sci. 50(6) (1995) 921–936.
[14] The Mathworks, Matlab Application Toolbox: Symbolic Math, 1997.